CB Report 338

$\bar{p}p \to \eta\eta$ and $\eta\eta'$ from 600 to 1940 MeV/c

A.V. Sarantsev and D.V. Bugg

Abstract. Data on $\bar{p}p \to \eta\eta$ and $\eta\eta'$ are presented from 600 to 1940 MeV/c. A partial wave analysis is made, adding these data to those for $\pi^0\pi^0$ at the same beam momenta. The $f_0(2100)$ appears strongly in the $\eta\eta$ channel with mass and width consistent with earlier data. The known $f_4(2050)$ and $f_4(2300)$ are observed, and also f_2 resonances at 2010 MeV and ~ 2300 MeV.

1 Introduction

Data on these channels were processed with identical procedures to $\pi^0\pi^0$. We therefore refer you to Technical Report 337 on $\bar{p}p \to \pi^0\pi^0$ for details of software which has been used and for $\pi^0\pi^0$ results. We shall report results for $\eta\eta$ and $\eta\eta'$ channels using both 4γ and 8γ events. The 4γ data for $\eta\eta$ are superior statistically by a factor 5–6 compared with 8γ, and have lower backgrounds. Therefore for $\eta\eta$ we use 8γ events only as a cross-check that angular distributions and normalisations come out in agreement with 4γ data. The physics is obtained purely from 4γ data. For $\eta\eta'$, the 8γ data have slightly higher statistics than 4γ, but also slightly higher backgrounds. We combine these two data sets to extract physics. Numbers of events are listed in Table 1 after background subtractions described below.

2 Selection Criteria

For $\eta\eta \to 4\gamma$, the following cuts are applied on confidence levels (CL): (i) $CL(\pi^0\gamma\gamma) < 0.1\%$, to remove $\pi^0\pi^0$, (ii) $CL(\pi^0\eta) < 0.01\%$, to remove $\pi\eta$, (iii) $CL(\eta\eta) > CL(\eta\eta')$. In the few cases where more than one $\eta\eta$ combinatoric solution is found, events are required to have CL at least a factor 10 better than the second solution. After these cuts, the Monte Carlo simulation predicts that background in the $\eta\eta$ sample will be $\leq 0.7\%$; sources of background at 1800 MeV/c are shown in Table 2 and are similar at lower momenta. It is isotropic within errors and is subtracted under this assumption. Wrong combinations of photons into η are predicted in 0.6% of events. Fig. 1(a) shows the $\gamma\gamma$ mass distribution close to the η, after these cuts have been

Momentum (MeV/c)	$\eta\eta \to 4\gamma$	$\eta\eta' \to 4\gamma$	$\eta\eta' \to 8\gamma$
600	638	33	65
900	7196	152	272
1050	7061	161	205
1200	8823	288	438
1350	4777	183	298
1525	3027	130	151
1642	3613	130	152
1800	4871	181	221
1942	5627	217	226

Table 1
Numbers of events at each momentum.

Channel	Background(%)		
	$\eta\eta$	$\eta\eta' \to 4\gamma$	$\eta\eta' \to 8\gamma$
$\eta\pi^0\pi^0$	0.5	5.0	-
$\eta\omega$	0.1	0.4	-
$\eta\eta$	0	0.3	-
$\omega\pi^0\pi^0$	0	0.8	-
$\pi^0\eta$	0	0.7	
$\eta\pi^0\pi^0\pi^0$	-	-	6.3
$\omega 3\pi^0$	-	-	2.7
$\eta 3\pi^0$	-	-	1.2
$\omega\eta\pi^0\pi^0$	-	-	0.8
$\eta 4\pi^0$	-	-	0.4
Other	0.1	0.9	0.5
Total	0.7	8.1	11.9

Table 2
Estimated sources of background at 1800 MeV/c in $\eta\eta \to 4\gamma$, $\eta\eta' \to 4\gamma$ and 8γ.

applied to events fitting $\eta\gamma\gamma$. The background under the second η is $\sim 1\%$, in close agreement with the Monte Carlo simulation.

A cross-check is that $\eta\eta$ data may be reconstructed also from 8γ events, where

one $\eta \to \gamma\gamma$ and the second $\eta \to 3\pi^0$. The $\eta 3\pi^0$ events need to be isolated from backgrounds arising from $4\pi^0$ and $\eta\eta\pi^0\pi^0$ and $\omega 3\pi^0$, $\omega \to \pi^0\gamma$. Confidence level cuts are: (i) $CL(\eta 3\pi^0) > 5\%$, (ii) $CL(4\pi^0) < 0.01\%$, (iii) $CL(\eta 3\pi^0) >$ 10 times that of other 4-body channels. Fig. 1(b) shows the mass distribution of $3\pi^0$ in the $\eta 3\pi^0$ sample. There is a strong $\eta \to 3\pi^0$ peak, from which we deduce angular distributions for $\eta\eta$ final states; sidebands are used from the region displayed in Fig. 1(b) to subtract the small background under the η signal.

For $\eta\eta'$ we derive comparable statistics from 4γ events where $\eta' \to \gamma\gamma$ and 8γ events where $\eta' \to \eta\pi^0\pi^0$. Background levels are also similar. For 4γ events, the selection criteria are: (i) $CL > 10\%$, (ii) $CL(\pi^0\gamma\gamma) < 0.1\%$, to remove $\pi^0\pi^0$, (iii) $CL(\pi^0\eta) < 0.01\%$, to remove $\pi^0\eta$, (iv) $CL(\eta\eta') > 10 * CL(\eta\eta)$. If there is more than one $\eta\eta'$ combinatoric solution, a factor > 100 difference in confidence level is required. Fig. 1(c) illustrates the level of background under the η' signal at one momentum after these cuts. The background level is on average 10%, and is isotropic within errors. Finally, in order to constrain events tightly to the η' peak, we require a CL at least 25% better than for $\eta\gamma\gamma$. The background agrees closely with that estimated from the Monte Carlo simulation of all other channels. Contributions to the background are shown in Table 1 and total $\sim 8\%$, marginally below that observed.

The 8γ events are selected demanding exactly 8 photons and a 5% confidence level cut for $\eta\eta\pi^0\pi^0$. Further requirements are: (i) $CL(4\pi^0) < 0.01\%$, to remove $4\pi^0$, (ii) $CL(\eta\eta\pi^0\pi^0)$ at least a factor 10 better than any other 8γ channel, (iii) $CL(\eta\eta')$ a factor 100 better than any combinatoric alternative. Fig. 1(d) then shows the mass distribution from $\eta\pi^0\pi^0$ combinations. There is a clear η' peak, from which angular distributions are derived requiring $M^2(\eta\pi\pi)$ between 0.887 and 0.95 GeV^2. A side-band estimate of background is made around the η' and is isotropic within errors; it is subtracted with that assumption. The background level is typically 15%, marginally above the Monte Carlo simulation, which estimates the backgrounds shown in Table 1 amounting to 12%. We have decided to take the average of data and Monte Carlo estimates of background and subtract 13.5% isotropic background.

Confidence level distributions for $\bar{p}p \to \eta\eta$ and $\eta\eta'$ in 4γ events are shown in Fig. 2 AFTER applying cuts to remove other channels. These cuts are responsible for making confidence level distributions far from flat. As for $\pi^0\pi^0$, the $\eta\eta$ angular distributions vary by insignificant amounts as the confidence level cut is varied over a wide range from 5 to 20%.

The effect of the background subtractions is to move differential cross sections uniformly downwards for all $\cos\theta$, hence deepening any dips in the data. In practice, the subtraction has negligible effect on physics conclusions. We have carried out the full amplitude analysis with and without background sub-

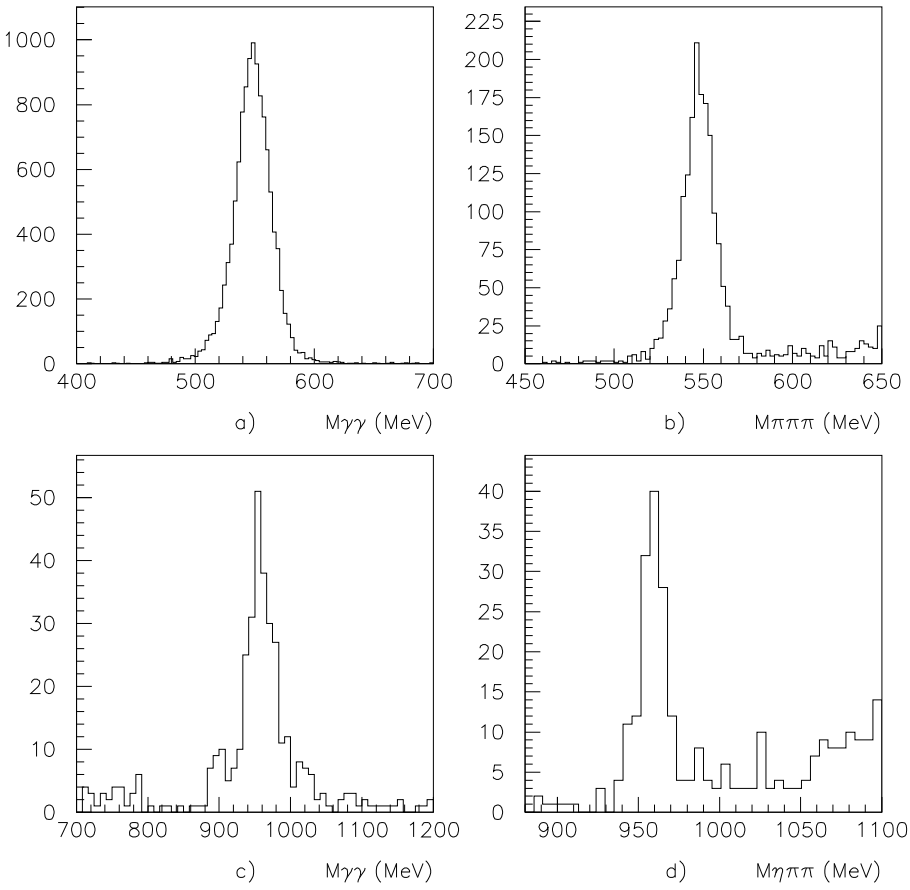

Fig. 1. Illustration of backgrounds under the η at 1800 MeV/c after cuts described in the text, in (a) 4γ data, (b) 8γ, and under the η' in (c) 4γ data, (d) 8γ. The region shown is used for background subtraction

.

traction, and conclusions about resonance hardly change at all; only coupling constants change slightly.

3 Comparison of 4γ with 8γ for $\eta\eta$

A cross-check is that $\eta\eta$ data may be reconstructed from 8γ events, where one $\eta \to \gamma\gamma$ and the second $\eta \to 3\pi^0$. Fig. 3 compares $\eta\eta$ angular distributions, as a function of centre of mass scattering angle θ, from 4γ events (black circles) and 8γ (open triangles). Within the statistics of the latter, there is good agreement

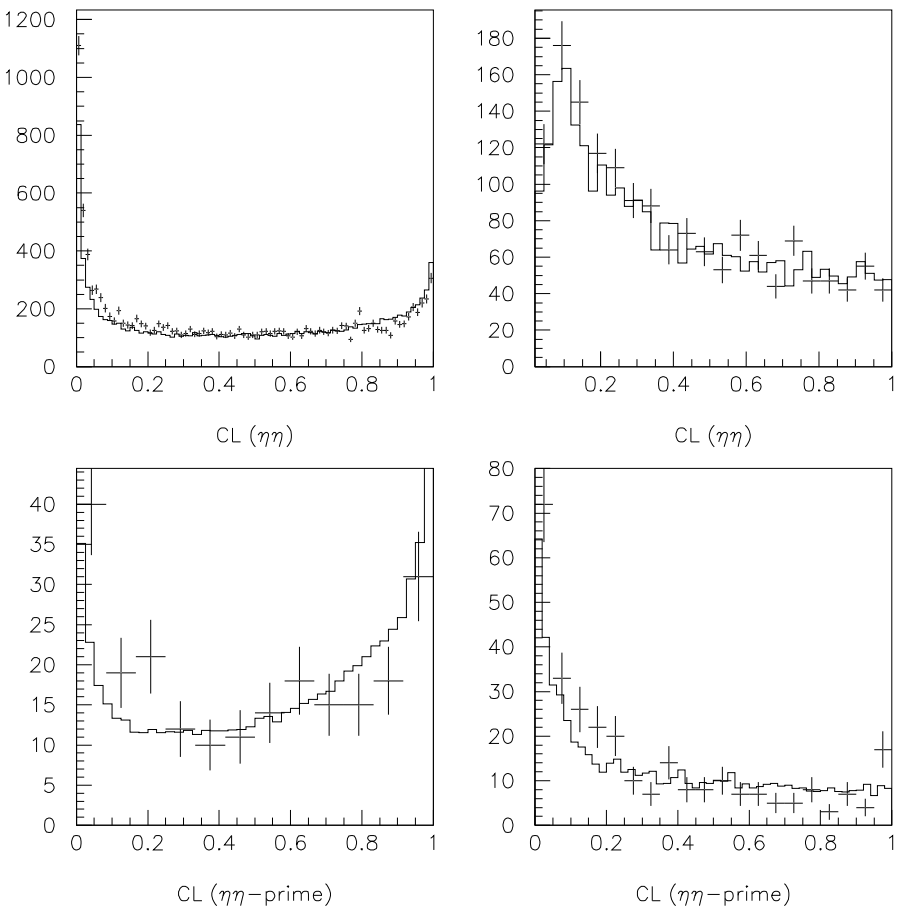

Fig. 2. Confidence level distributions for (a) $\eta\eta$ from 4γ data (top left), (b) $\eta\eta$ from 8γ data (top right), (c) $\eta\eta'$ from 4γ data (bottom left) and (d) $\eta\eta'$ from 8γ data (bottom right). Histograms show predictions from the Monte Carlo AFTER the application of multiple cuts to suppress background.

for both the shape of the angular distribution and the absolute magnitude of the cross section, shown on Fig. 4. This checks the reliability of the Monte Carlo estimation of the efficiency of reconstruction.

For $\eta\eta'$, we find that the normalisation of 8γ data is everywhere slightly below that of 4γ data. However, the branching ratio of $\eta' \to \gamma\gamma$ has an error of $\pm 6\%$ and that for $\eta' \to \eta\pi^0\pi^0$ has an error of $\pm 6.5\%$. For the relative branching ratio between $\gamma\gamma$ and $\eta\pi^0\pi^0$, the Particle Data Group [1] quotes an error of $\pm 7\%$ for their fit and $\pm 9.5\%$ for their average. In order to get the best agreement between 4γ and 8γ, we need to scale 4γ data down by 5% and 8γ up by 5%,

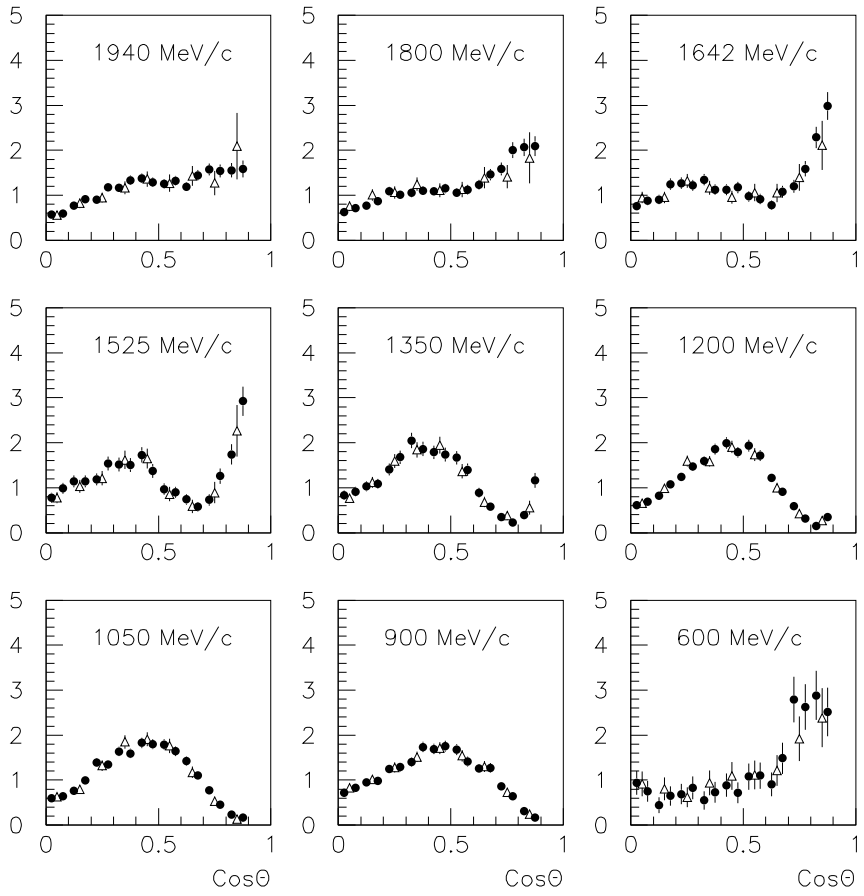

Fig. 3. Comparison of angular distributions for $\eta\eta$ from 4γ events (black circles) and 8γ (open triangles).

i.e. roughly a 1σ change in the relative branching ratios. After this change, Fig. 5 compares angular distributions for $\eta\eta'$ from 4γ and 8γ. The agreement is as good as may be expected with the available statistics. Fig. 6 shows a comparison of the integrated cross sections for 4γ and 8γ data after the 10% renormalisation.

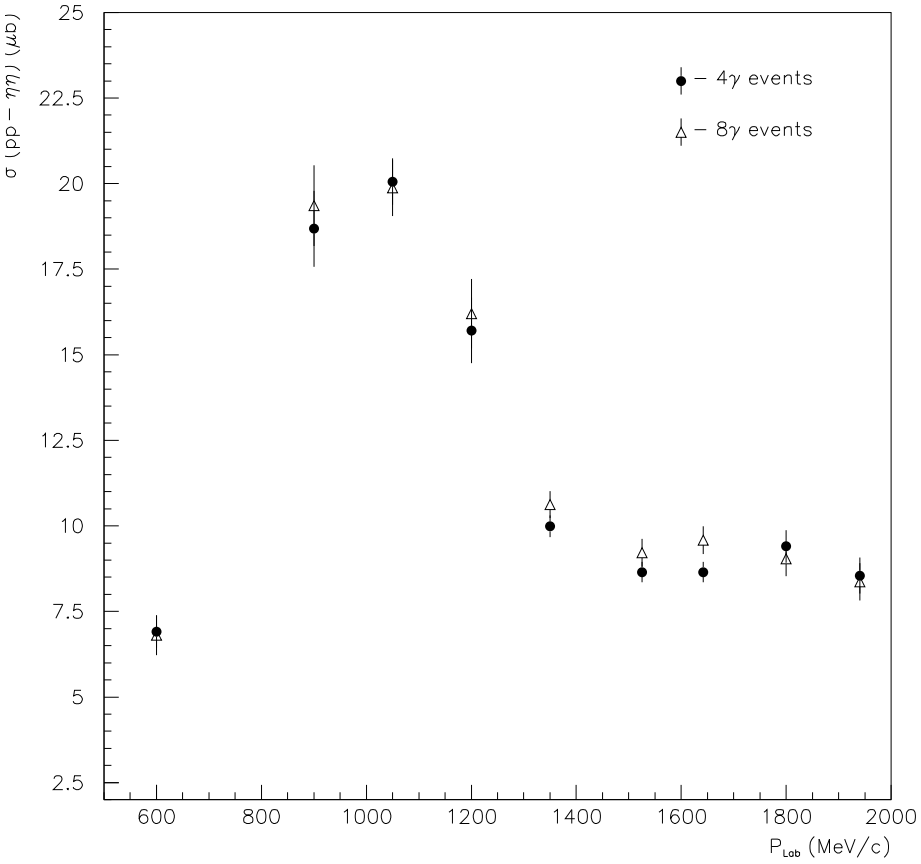

Fig. 4. Comparison of integrated cross sections for $\eta\eta$ from 4γ events (black circles) and 8γ (open triangles).

4 Results

Resulting angular distributions for $\eta\eta$ and $\eta\eta'$ are shown in Figs. 7 and 8, where they are compared with fits. The normalisation has been corrected to allow for all decay modes of the η and η'. Dotted curves illustrate the acceptance. It falls rapidly around $\cos\theta = 0.85$ and we discard the few events beyond $\cos\theta = 0.9$.

Fig. 9 shows cross sections for $\eta\eta$ and $\eta\eta'$ integrated from $\cos\theta = 0$ to 0.85. Curves show the fits from solution 2 (full curve) and solution 1 (dashed).

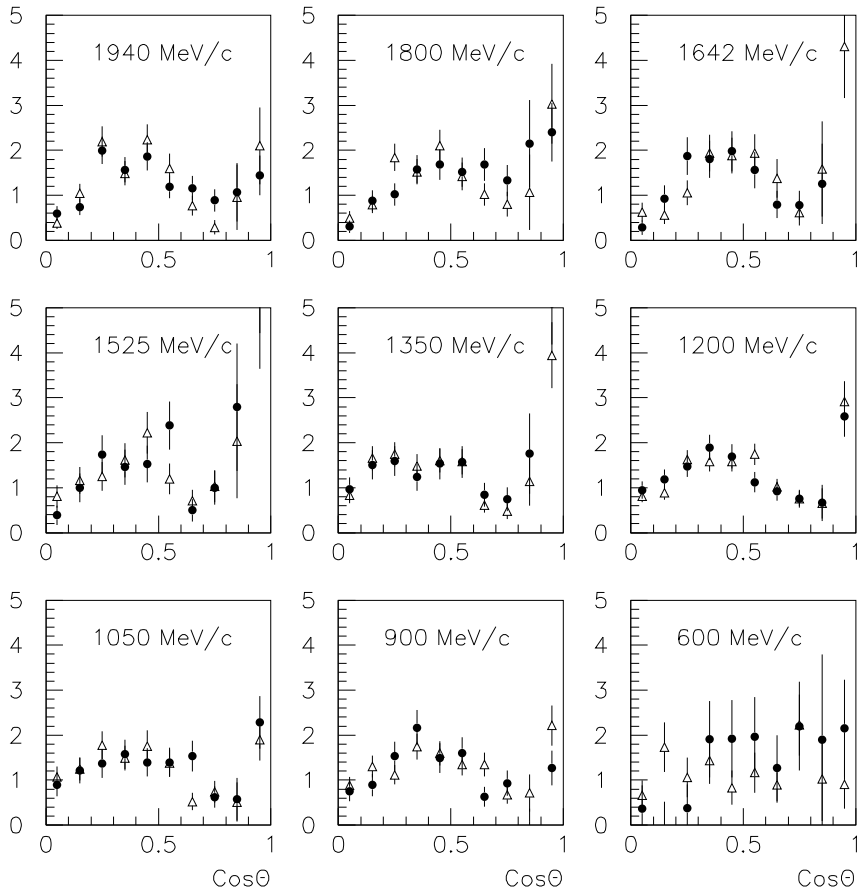

Fig. 5. Comparison of angular distributions for $\eta\eta'$ from 4γ events (black circles) and 8γ (open triangles) at four momenta.

5 Partial wave analysis

Formulae for differential cross sections in terms of partial waves have been given by Hasan and Bugg [2] and are repeated in CB report 337 on $\bar{p}p \to \pi^0\pi^0$. We fit the data in terms of a sum of s-channel resonances. Even if t-channel exchanges are present, partial wave amplitudes will acquire a phase variation from these resonance by Watson's theorem. That is, the amplitudes must share the Breit-Wigner denominator.

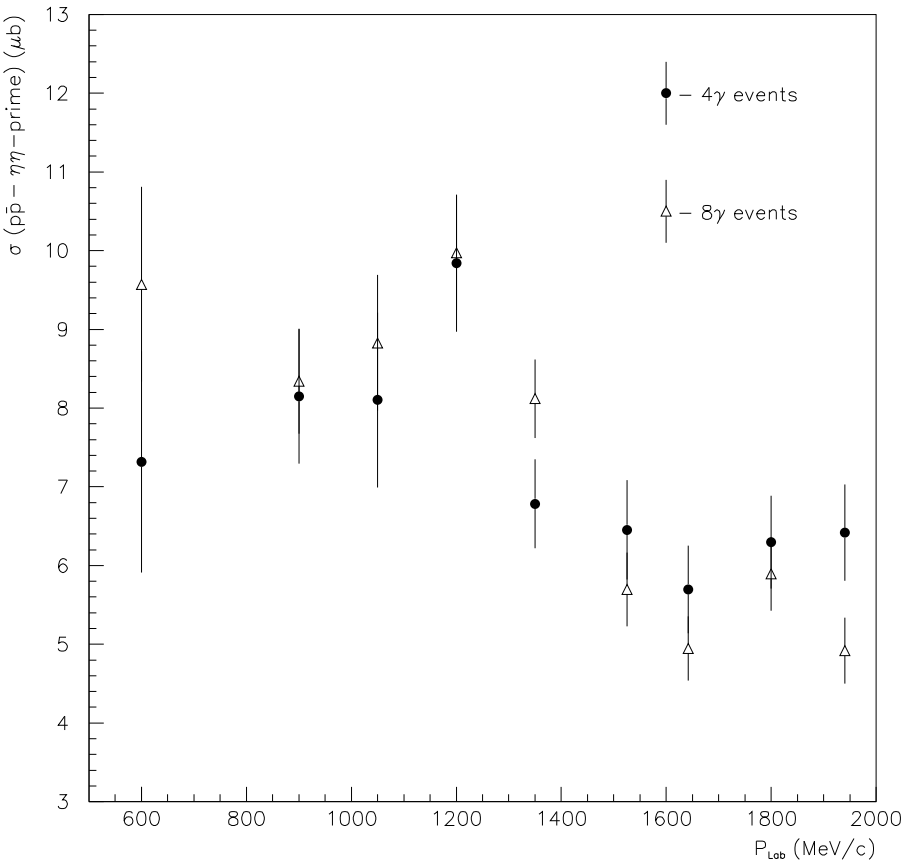

Fig. 6. Comparison of integrated cross sections for $\eta\eta'$ from 4γ events (black circles) and 8γ (open triangles), after renormalisation the relative branching ratios of $\eta' \to \gamma\gamma$ and $\eta' \to \eta\pi^0\pi^0$ by 10%.

We find it essential to include as a minimum two 4^+ resonances, two 2^+ plus a broad background, and one 0^+ resonance plus a background. The backgrounds are parametrisesed as broad resonances. They provide more flexibility to the background than a simple constant. For 0^+, the pole position lies far below threshold in solution 2 described below and the fit is insensitive to its precise mass and width. In solution 1 there is no background. For 2^+, it is interesting that the mass optimises naturally in the region 1850–1950 MeV and the width in the range 350–500 MeV. These parameters are consistent with the broad 2^+ signal we observed in the $\eta\eta$ channel in $\eta\eta\pi^0$ data from 1350 to 1940 MeV/c [3]. The χ^2 of the fit changes very little if the mass is fixed at 1980 MeV and the width at 500 MeV, the optimum parameters from [3].

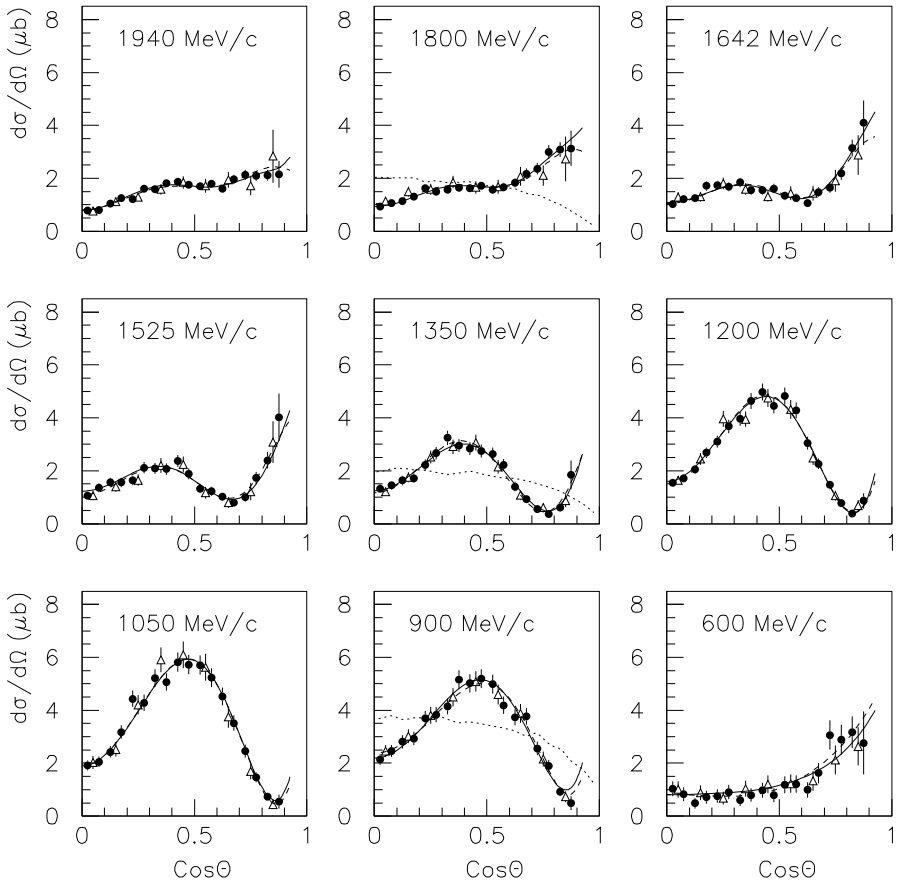

Fig. 7. Angular distributions for $\bar{p}p \to \eta\eta$ compared with the fit of Table 3 for solution 1 (dashed curves) and solution 2 (full curves). Dotted curves illustrate the acceptance.

The T-matrix for each partial wave is parametrised as:

$$T_{L,J} = \sum_i \frac{G_i B_L(p) B_J(q)}{s - M_i^2 - i M_i \Gamma_i}, \tag{1}$$

where G_i are complex coupling constants, $B_L(p)$ is the standard Blatt-Weisskopf centrifugal barrier in terms of the momentum p in the $\bar{p}p$ channel, and $B_J(q)$ is the centrifugal barrier in terms of the momentum q in the $\pi\pi$ channel. This parametrisation imposes the important constraint of analyticity. Unitarity is

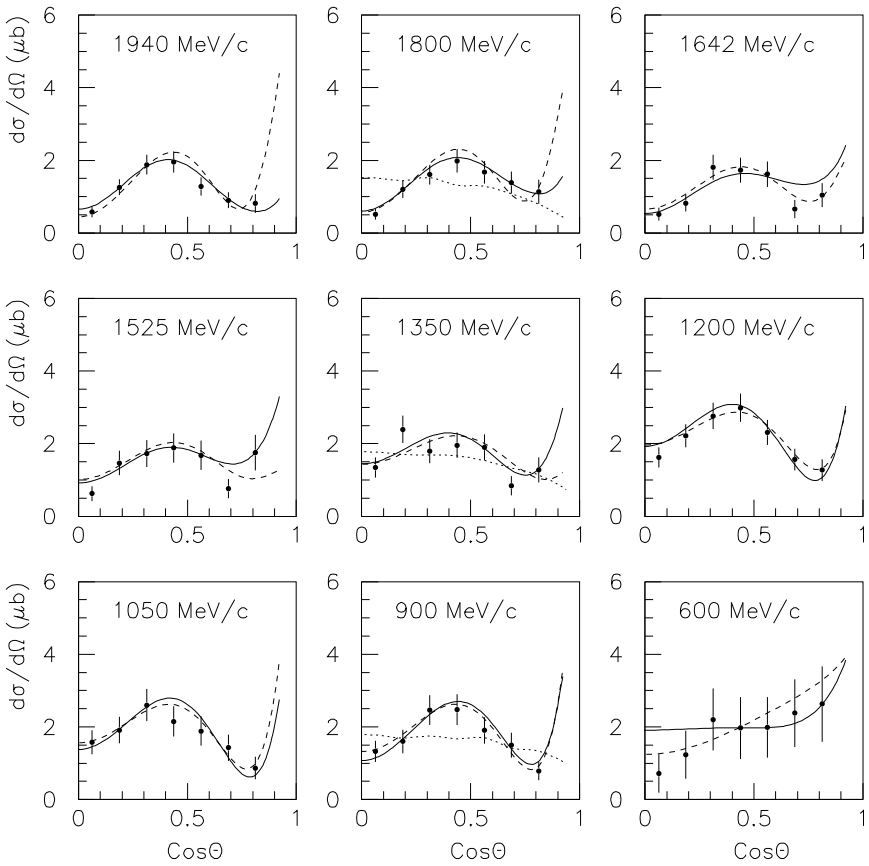

Fig. 8. Angular distributions for $\bar{p}p \to \eta\eta'$ compared with the fit of Table 3 for solution 1 (dashed curves) and solution 2 (full curves). Dotted curves illustrate the acceptance.

irrelevant, since the amplitudes are far below the unitarity limit, and we know nothing about the coupling to many channels. Ratios of coupling constants of each resonance to $^3P_2$ and $^3F_2$ are fixed to be the same for $\pi\pi$, $\eta\eta$ and $\eta\eta'$, since these ratios are a property of the entrance $\bar{p}p$ channel. However, interferences of resonances with the broad backgrounds affect strongly the intensities oberved in $^3P_2$ and $^3F_2$ channels in Fig. 10 below.

We have carried out fits (a) to $\eta\eta$ data alone, (b) to $\eta\eta$ and $\pi^0\pi^0$ together, (c) to $\eta\eta$ and $\eta\eta'$, (d) ultimately to $\pi^0\pi^0$, $\eta\eta$ and $\eta\eta'$. There are no significant

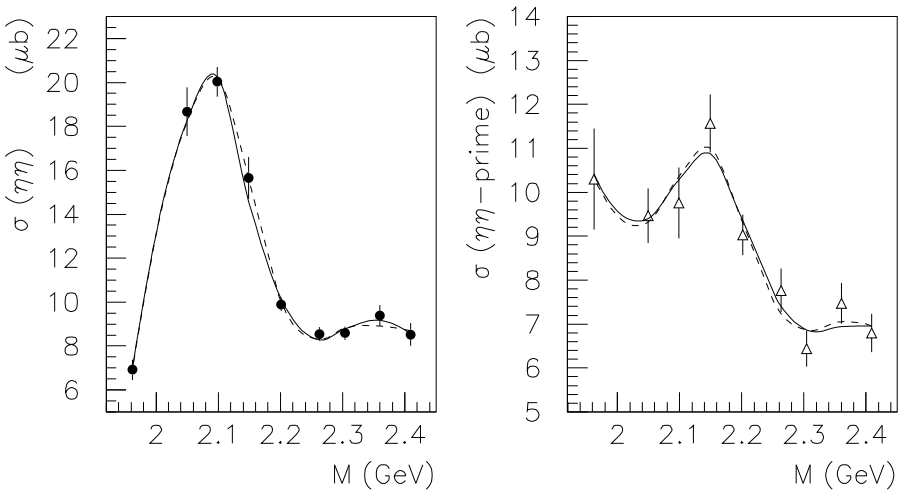

Fig. 9. Cross sections integrated from $\cos\theta = 0$ to 0.85 for (a) $\bar{p}p \to \eta\eta$, (b) $\bar{p}p \to \eta\eta'$, compared with solutions 1 (dashed) and solution 2 (full curve).

differences between these fits, hence no evidence for $s\bar{s}$ states.

The two distinct solutions we have reported in CB report 337 for $\pi^0\pi^0$ persist in fits to $\eta\eta$ and $\eta\eta'$. Intensities are shown in Fig. 10. We shall list several physics objections to solution 1. In addition to these objections, it does not 'feel' a good solution. Convergence is slow, and it is possible to find two nearby local mimima which collape to the solution we show, with improvements in χ^2 of 80–100, when they are perturbed sufficiently. The differences of these local minima to solution 1 lie mainly in $\eta\eta'$, where statistics are low.

Before discussing these solutions, we remark that we have tried applying constraints based on the wave functions of η and η' in terms of quarks:

$$\eta = 0.8|(u\bar{u} + d\bar{d})/\sqrt{2} > +0.6|s\bar{s} >, \tag{2}$$

$$\eta' = -0.6|(u\bar{u} + d\bar{d})/\sqrt{2} > +0.8|s\bar{s} > . \tag{3}$$

Here we use the Crystal Barrel value of the pseudo-scalar mixing angle, $\theta_{PS} = -17.3°$ [4]. If the s-channel resonances we observe are purely $(u\bar{u} + d\bar{d})/\sqrt{2}$, one expects coupling constants for $\pi^0\pi^0$, $\eta\eta$ and $\eta\eta'$ channels to be related by

$$G(\eta\eta) = 0.8G(\pi^0\pi^0) \tag{4}$$

$$G(\eta\eta') = -0.6G(\pi^0\pi^0) = -0.75G(\eta\eta). \tag{5}$$

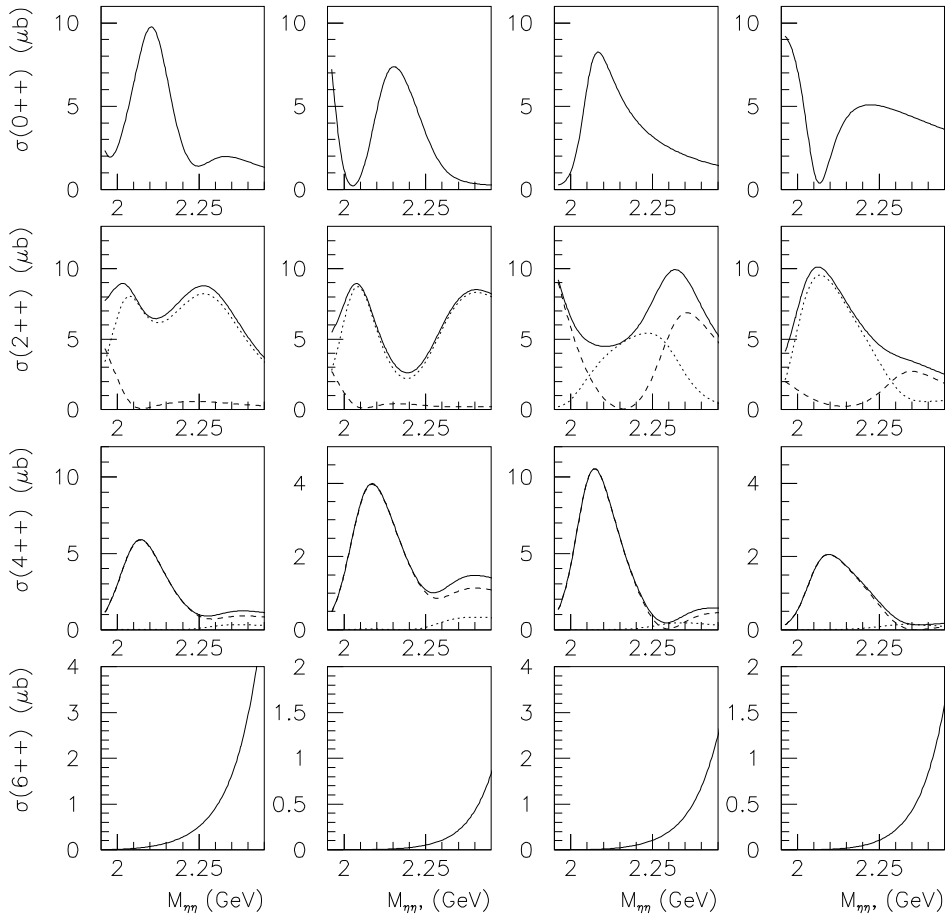

Fig. 10. Intensities fitted to $\eta\eta$ and $\eta\eta'$: solution 1 $\eta\eta$ column 1, $\eta\eta'$ column 1; solution 2 $\eta\eta$ column 3, $\eta\eta'$ column 4. Dashed curves show $^3P_2$ and $^3F_2$, dotted curves $^3F_2$ and $^3H_4$. Full lines show their sum. Interferences drop out of integrated cross sections.

The order of magnitude of $\eta\eta'$ differential cross sections in Fig. 8 is half that of $\eta\eta$ in Fig. 7; centrifugal barriers will suppress $\eta\eta'$ slightly. So, globally, the cross sections are not far from the constraint of equn. (5). When one looks at details, it is clear that equn. (5) must be violated somewhere. The $\eta\eta$ cross sections are globally about 20% of $\pi^0\pi^0$, so there is a larger discrepancy with equn. (4). Nonetheless, we find that the data resist strongly any attempt to fit individual resonances to the constraints of either equn. (4) or (5).

This result is not surprising. One anticipates a 2^+ glueball in this mass range,

J^P	M (MeV/c^2)	Γ (MeV/c^2)	M (MeV/c^2)	Γ (MeV/c^2)
4^+	2044	208	2044	208
4^+	2295 ± 15	230 ± 20	2290 ± 10	230 ± 25
2^+	2010 ± 20	180 ± 35	2015 ± 20	190 ± 40
2^+	2295 ± 15	265 ± 85	2305 ± 15	225 ± 30
0^+	2090 ± 25	180 ± 40	2090 ± 30	185 ± 35
0^+	2250 ± 20	220 ± 35	-	-
0^+	1945 ± 20	90 ± 35	-	-

Table 3
Masses and widths of fitted resonances; columns 2 and 3 show solution 1 and columns 4 and 5 solution 2.

and it is likely to mix states strongly. If the 0^+ glueball has a very broad component $f_0(1530)$ as Anisovich and Sarantsev claim [5], there will be similar mixing for 0^+ states. Thirdly, it seems likely that t-channel exchanges will act as driving forces. The couplings of $N\bar{N}$ and $N\bar{\Delta}$ to $\pi\pi$, $\eta\eta$ and $\eta\eta'$ are quite different and will disturb the SU(3) constraints. We have tried to impose equns. (4) and (5) for 4^+ states only, but even this fails dramatically. If applied only to $f_4(2050)$ in a combined fit to $\pi^0\pi^0$ and $\eta\eta$, χ^2 rises from 594 to 1545 for just one additional constraint. Our conclusion is that coupling constants must be fitted freely.

6 Resonances

The minimum set of resonances giving an acceptable fit is shown in Table 3. The χ^2 is 408 for solution 1 and 429 for solution 2. There are 387 differential cross sections which are normalised to 27 integrated cross sections; there are 73 fitted parameters for solution 1, or 65 for solution 2. All resonances of Table 3 are required strongly. We have tried omitting each in turn from $\pi\pi$, $\eta\eta$ or $\eta\eta'$ or all of them; in this operation, all masses and width and coupling constants are re-optimised. The resulting changes in χ^2 are shown in Table 4. All resonances are highly significant.

The mass and width of $f_4(2050)$ are constrained to PDG values and the radius of the centrifugal barrier optimises at a reasonable value of 0.92 fm from the position of the peak in the 4^+ intensity. The peak of the $f_4(2050)$ is shifted up to ~ 2090 MeV in Fig. 10 by the strong effect of the centrifugal barrier in the $\bar{p}p$ channel. If the width is fitted, it optimises at 178 ± 9 MeV.

The $f_4(2300)$ appears as a shoulder in $\pi\pi$ data in solution 2 and as a peak

Solution	Resonance	$\pi\pi$	$\eta\eta$	$\eta\eta'$	All
1	$f_4(2050)$	52	119	18	670
	$f_4(2300)$	101	19	7	369
	$f_2(2005)$	168	16	12	241
	$f_2(2295)$	101	54	20	223
	$f_0(2100)$	2	138	6	160
	$f_0(2250)$	89	76	10	254
	$f_0(1945)$	1015	72	111	1309
2	$f_4(2050)$	160	749	108	937
	$f_4(2300)$	1244	108	4	2239
	$f_2(2005)$	557	144	0	1167
	$f_2(2300)$	201	167	20	382
	$f_0(2100)$	31	170	40	248

Table 4
Changes in χ^2 when each resonance is omitted.

in $\pi^0\pi^0$ in solution 1. Solution 2 is close to that of Hasan and Bugg [2], Fig. 3. They fitted $\bar{p}p \to \pi^-\pi^+$ data which include polarisation information. The polarisation separates $^3F_4$ from $^3H_4$ and is therefore an extremely powerful constraint. Another pointer towards solution 2 arises in Bing Song Zou's analysis of $\eta\pi^0\pi^0$ data. His solution for 4^+ states resembles solution 2 closely in the relative strengths of $^3F_4$ and $^3H_4$. A third strong objection to solution 1 is that $f_4(2050)$ decays more strongly to $\eta\eta$ than to $\pi^0\pi^0$ by a factor 1.6. That contradicts entries in the Particle Data Tables, where three groups are quoted as observing strong $\pi\pi$ decays. The GAMS group observes much weaker decay to $\eta\eta$. A fourth objection to solution 1 is that it requires a narrow 0^+ resonance at 1945 MeV with a width of only 90 MeV; that seems physically implausible. For all these reasons we prefer solution 2, but we present solution 1 as a numerical possibility.

For $J^P = 2^+$, $\pi^0\pi^0$ data have a strong peak at 2020 MeV. It has a large $^3F_2$ component. Because of the $L = 3$ centrifugal barrier, the peak is pushed up noticeably and the pole position is at 2010 MeV. Solution 1 also requires an $f_2(2010)$ with a large $^3F_2$ component. Both solutions require $f_2(2010)$ in $\eta\eta'$.

Because of the proximity of this resonance to $f_4(2050)$ and also because of the strong coupling to $\bar{p}p\ ^3F_2$, it seems likely that this resonance is the expected $\bar{q}q\ ^3F_2$ state. The $\bar{q}q$ state will have a wave function peaking strongly at large r; in the absence of strong effects of the operator in the matrix element for

decay, the final state is then likely to have a large $L = 3$ component.

The $\eta\eta$ data demand a further 2^+ resonance around 2300 MeV. Without it, $\pi^0\pi^0$ and $\eta\eta'$ data are also poorly fitted.

For $J^P = 0^+$, both solutions requires a strong $f_0(2100) \to \eta\eta$. It always peaks in the mass range 2080-2100 MeV, though interference with the background 0^+ amplitude allows the pole position to drift over the range 2050–2115 MeV. The width tends to fit at a slightly lower value of ~ 180 MeV compared with the value 203 ± 10 MeV given by E760 [6].

7 Further Possible Resonances

Both Bing Song Zou's $\eta\pi^0\pi^0$ analysis and the present data are consistent with towers of $I = 0$ resonances at roughly 2020 and 2300 MeV. The $3\pi^0$ data likewise indicate towers of $I = 1$ resonances at similar masses; these will be reported shortly.

It therefore seems likely that there will be an additional 0^+ resonance at ~ 2300 MeV. Solution 1 definitely requires a 0^+ resonance at 2250 ± 20 MeV, with $\Gamma = 220 \pm 35$ MeV. We have tried adding a 0^+ resonance to solution 2 with $M = 2250 - 2300$ MeV, $\Gamma = 250$ MeV, then optimising all M, Γ. The χ^2 of the fit does improve by ~ 80, but the mass and width of the additional resonance are not well defined. Solutions are possible with M anywhere in the range 2180–2340 MeV. The width also tends to drift to an unreasonably low value of ~ 80 MeV unless it is constrained. We therefore regard the present evidence for this additional 0^+ state in solution 2 as inconclusive.

For $J^P = 2^+$, Bing Song Zou observes $f_2(2020)$ in agreement with present data. He observes two further 2^+ states at higher mass: an $f_2(2240 \pm 40)$ with $\Gamma = 170 \pm 50$ MeV, decaying dominantly to $f_2(1270)\pi$, and an $f_2(2370 \pm 50)$ with $\Gamma = 320 \pm 50$ MeV decaying dominantly to $a_2(1320)\pi$. One indeed expects both a $^3P_2$ and a $^3F_2$ state in this mass region. It is quite possible that the $f_2(2300)$ we fit is an unresolved mixture of these two states. We have tried adding a third 2^+ state and χ^2 improves by ~ 100. However, masses and widths of the two states are poorly determined. Their wave functions will be orthogonal. We have therefore tried fitting with two orthogonal sets of coupling constants. The solution is still poorly determined. For the moment, the evidence for an extra 2^+ state from the present data must be regarded as inconclusive.

8 Systematic errors

We have scanned the mass and width of every resonance one by one, re-optimising every parameter except the one being scanned; eg. when optimising the mass of resonance 1, say, the masses and widths of all other resonances are allowed to optimise, together with the width of resonance 1 and all coupling constants. In all cases, nice parabolic optimima are observed over a range of at least 50 MeV. Statistical errors on masses are typically 2–3 MeV and on widths are typically 5-10 MeV.

However, systematic errors are larger. We have estimated these systematic errors so as to cover the following variations: (i) applying SU(3) constraints to the coupling constants of the 6^+ amplitude, and varying the width of the resonance which describes it from 250 MeV by $\pm$100 MeV; (ii) constraining the mass and width of the broad 2^+ component to the range 1980 ± 50 MeV, $\Gamma = 500 \pm 100$ MeV, as found in our analysis of $\eta\eta\pi^0$ data from 1350 to 1940 MeV/c; (iii) changing the form of the 0^+ background; (iv) in solution 2, introducing an extra 0^+ resonance at 2300 MeV with width 250 MeV. Errors given in Table 3 cover these systematic variations, which have only modest effects on other components.

9 Branching ratios

We refrain from quoting branching ratios at present, since they depend in a delicate way on interferences with background amplitudes. Errors are typically $\pm$50% for individual components as one applies the systematic variations described in the previous section. However, the magnitudes of peaks in the intensities are more stable; they vary by typically $\pm$5–20%.

We draw attention to one startling result. The ratio of branching ratios $BR[f_4(2050) \rightarrow \eta\eta]/BR[f_4(2050) \rightarrow \pi\pi]$ is 0.047 ± 0.015 in our preferred solution 2; this is a factor 4 higher than the GAMS result quoted by the PDG: 0.0012 ± 0.005. Our error covers systematic errors arising from the interaction between $f_4(2050)$ and $f_4(2300)$. For solution 1, the ratio is 0.47, a factor 40 larger than the GAMS result; that seems beyond the realms of credibility.

We have tried constraining the fit to $\eta\eta$ data to the GAMS branching ratio, but the fit is worse in χ^2 by 116 and visibly poorer for $\eta\eta$ in the mass range around 2050-2100 MeV. We have access to the GAMS data and, when time permits, we shall refit them to form our own opinion of this branching ratio. Presently they quote two solutions; there might be others. They assume pion exchange, and this might affect the determination of overall cross sections.

10 Summary

The $\pi^0\pi^0$, $\eta\eta$ and $\eta\eta'$ data may be fitted simultaneously with acceptable χ^2. Both solutions require (i) $f_4(2050)$, (ii) $f_4(2300)$ with $M = 2295 \pm 15$ MeV, $\Gamma = 230 \pm 25$ MeV, (iii) $f_2(2010 \pm 20)$ with $\Gamma = 180 \pm 35$ MeV, (iv) an f_2 around 2300 MeV and (v) $f_0(2100)$ with mass and width consistent with earlier data. Solution 1 seems unlikely for four reasons, the strongest of which is that it requires $f_4(2050)$ to decay weakly to $\pi\pi$ and more strongly to $\eta\eta$, in conflict with earlier data from several experiments. Solution 2 looks similar to the earlier analysis of Hasan and Bugg, which has the advantage of including polarisation data. It also resembles the solution found by Bing Song Zou for $\eta\pi^0\pi^0$ data.

References

[1] Particle Data Group, Euro. Phys. J. 3(1998) 1.

[2] A. Hasan and D.V. Bugg, Phys. Lett. B334 (1994) 215.

[3] A. Anisovich et al, eta-eta-pizero paper, 1350–1940 MeV/c, to be submitted to Phys. Lett. B.

[4] C. Amsler et al., Phys. Lett. B294 (1992) 451.

[5] A. Anisovich et al., Z. Phys. A357 (1997) 173.

[6] T.A. Armstrong et al., Phys. Lett. B307 (1993) 394.